LAMINAR NATURAL CONVECTION OF NON-NEWTONIAN POWER-LAW FLUID IN AN ECCENTRIC ANNULUS

by

***Oussama BENHIZIA*[a*], *Mohamed BOUZIT*[b], *and Ahmed Zineddine DELLIL*[a]**

[a] Department of ELM, Institute of Maintenance and Industrial Safety, University of Oran 2 Mohamed ben Ahmed, Oran, Algeria
[b] University Centre Belhadj Bouchaib, Ain Temouchent, Algeria

Original scientific paper
https://doi.org/10.2298/TSCI190805424B

This work is about studying the natural convection of 3-D steady-state non-Newtonian power law fluid numerically. The inner cylinder was put eccentrically into the outer one. The cylinders are held at constant temperatures with the inner one heated isothermally at temperature, T_h, and the outer one cooled isothermally at temperature T_c ($T_h > T_c$). The simulations have been taken for the parameters $10^3 \leq Ra \leq 10^5$, $10 \leq Pr \leq 10^3$, $0.6 \leq n \leq 1.4$, and $0 \leq \varepsilon \leq 0.9$, and an inclination angle, ϕ, from 0° to 90°. The average Nusselt numbers for the previous parameters are obtained and discussed numerically. The results revealed that the average Nusselt number has the highest values when $n = 0.6$, $Ra = 10^5$ at $\phi = 0$ which is a signal for the large transfer herein and has the lowest values for $n = 1.4$, $Ra = 10^3$, at $\phi = 90°$ which is a signal that the transfer is by conduction more than convection. Furthermore, the increasing of eccentricity causes an increase in the Nusselt number for all the cases. Finally, the best case where we can get the best heat transfer is at $\phi = 0$, $\varepsilon = 0.9$ among them all. The results have compared with some precedent works and showed good agreement.

Key words: *natural convection, eccentric annulus, ANSYS CFX, non-Newtonian fluid, power law model, Nusselt number*

Introduction

In fluid dynamics, the Taylor-Couette flow consists of a viscous fluid confined in the gap between two rotating cylinders. For low angular velocities, measured by the Reynolds number, the flow is steady and purely azimuthal (when the cylinders are stationaries there is a natural convection measured by the Rayleigh number). It has many technical apparatus like scraped surface heat exchangers, shear crystallizers because of its unique flow characteristics, desalination, MHD and also in viscosimetric analysis.

Natural convection between two eccentric cylinders has been one of the subjects of many researchers in the last few years due to its importance in many engineering applications such as solar collectors, nuclear reactors, cooling of electronic systems, and heat exchangers. One of the earliest works in this field was done by Mack and Bishop [1], they studied the issue of natural convection in a concentric annulus at low Rayleigh numbers (less than or equal 10^3) and radius ratio $1.15 \leq R_o/R_i \leq 4.15$ and represented the temperature variables and stream function. Kuehn and Goldstein [2] investigated the issue of natural convection in a concentric and eccentric cylindrical annuli. They performed experimental and numerical studies of the problem

* Corresponding author, e-mail: benhizia_oussama@yahoo.fr

and their results are used to validate most of the numerical works nowadays. Char and Lee [3] studied the natural convection of micropolar fluids in a horizontal eccentric annulus numerically. They figured out that the inversion parameter and the eccentricity have a strong effect on the flow structure and heat transfer rate.

Kim *et al.* [4] studied the natural convection of power law fluid in an enclosure in the presence of magnetic field. They demonstrated that the power law index, n, largely influences the heat and mass transfer and average entropy generation. Naimi *et al.* [5] carried out a study for the steady-state buoyancy driven flow of a non-Newtonian power law fluid in a rectangular horizontal annulus where it was heated from below. The effects of Prandtl and Rayleigh numbers, the power law index, n, and aspect ratio on the stream function and Nusselt number are investigated. Sakr *et al.* [6] carried out experimental and numerical studies on natural convection in a gap between two cylinders formed by a constant heat flux, the inner (elliptic) horizontal cylinder was put concentrically into a larger isothermally cooled horizontal cylinder. The simulations covered ranges of $1.12 \cdot 10^7 \leq \mathrm{Ra} \leq 4.92 \cdot 10^7$, orientation angle of the elliptic tube $0° \leq \phi \leq 90°$ and hydraulic radius ratio $1.5 \leq R_\mathrm{o}/R_\mathrm{i} \leq 6.4$. The numerical results compared with the experiment ones and showed good agreement.

The comparison between the convective transport by temperature and by heat flux in an annulus and in a cavity for power-law fluid was done by [7, 8], respectively. Their results indicated that the increase in the transfer rate is greater when the convective transport is by heat flux rather than the Rayleigh number based on the same temperature difference; However, for large diameter ratios ($RR \geq 10$) the heat transfer rates are the same for both types of heating.

Abu-Nada, *et al.* [9] studied the heat transfer in horizontal annuli using Cu-, Ag-, Al_2O_3- and TiO_2-water nanofluids with different volume fractions. They found that the nanofluid type and volume fraction have too much effect on the heat transfer characteristics at high Rayleigh numbers and big values of diameter ratio, but for intermediate values of Rayleigh number, the nanofluid has low solid thermal conductivity which caused a decrease in heat transfer rate. The effect of an inclination angle on natural convection [10, 11] power-law fluid [12] in a square enclosure has been investigated. The authors presented isotherms and streamlines of the vorticity-stream function procedure, effects of the various parameters on the average Nusselt number and they accomplished a correlation of the Nusselt number based on the governing parameters as well. Parvin *et al.* [13] studied the steady-state free convection of Al_2O_3-water nanofluid in an annulus using Chon and the Maxwell Garnett models to estimate the heat transfer enhancement in the annulus. They found out that the heat transfer developed better by increasing the nanoparticles volume fraction and Prandtl number at moderate and large Grashof number for both models but the greatest heat transfer rate is found for the Chon model. Chhabra *et al.* [14] carried out a simulation of the free convection heat transfer of Bingham fluid in horizontal concentric cylinders under the conditions of $10^2 \leq \mathrm{Ra} \leq 10^6$, $30 \leq \mathrm{Pr} \leq 100$, and $0 \leq \mathrm{Bn} \leq 10^4$. They represented isotherms and streamlines contours for the numerical domain, local and average Nusselt numbers for the various parameters obtained and discussed as well.

The effects of buoyancy driven flow on the Nusselt number for power-law fluid [15] and the analysis of unsteady-state natural convection [16, 17] and the mixed convection over square cylinders [18, 19] have been studied numerically. They found that the heat transfer rate of pseudo-plastic fluid is much higher than the Newtonian fluid and for dilatant fluid heat transfer rate is less than the Newtonian one. Also, the Richardson number has an important role on the flow pattern and the heat transfer characteristics. Matin *et al.* [20] studied numerically the effects of the parameters Ra, Pr, aspect ratio, AR, eccentricity, ε, and power law index, n, on the natural convection of non-Newtonian power law fluid in two eccentric square ducts. They presented streamlines, isotherms and Nusselt numbers for the previous parameters, they proved that the Nusselt number is high when index n is low and vice versa, Prandtl number has almost no effect on the heat transfer characteristics.

Alawi *et al.* [21] studied the natural convection of SiO_2 nanofluid formed by constant heat flux horizontal inner flat tube concentrically had been put in cooled outer horizontal cylinder. The study of free convection of Cu-water nanofluid in an odd shaped cavity and in a gap of two heated confocal elliptic cylinders was done by [22, 23], respectively. Effects of the parameters Ra, volume fraction and hydraulic diameter ratio on the average Nusselt number are discussed. The simulation of the natural convection inside a cavity of two isothermal horizontal walls and two adiabatic side walls of power law fluid [24] and nanofluids [25, 26] has been studied in the past few years. The authors introduced a correlation for the mean Nusselt number *vs.* the Rayleigh number, Prandtl number, the power law index, and nanoparticles volume fraction. The influence of buoyancy on heated cylinder at mixed convection for Bingham plastic fluid [27] and effects of variable viscosity property of Al_2O_3-water nanofluid [28, 29] on the heat transfer characteristics are studied numerically. The results said when increasing Re, Pr, Bn, R_i, the momentum and thermal boundary-layers become thinner over the cylinder. Also, the pressure coefficient, the drag coefficient, the volume fraction and the mean Nusselt numbers are discussed. Another important geometries are:

– A square domain (porous cavity) heated by a triangular thick wall [30, 31] filled with nanofluid and a triangular wall with an opening from the top [32]. These studies presented isotherms and streamlines for different parameters such as Rayleigh number, wall thickness, nanoparticles volume fraction… and their influences on the Nusselt numbers.
– An enclosure of wavy walls is being studied for natural convection [33] and mixed convection [34]. Both papers showed the maps of heat transfer in the numerical domain as isotherms and streamlines and revealed that the amplitude of the wavy walls largely affects the heat transfer and fluid-flow.

From the mentioned literature, the natural convection of non-Newtonian power law fluids in square ducts and in a gap between two concentric cylinders has been investigated. Yet there is no study related to the natural convection of power law fluids in eccentric gaps. Since the natural convection inside eccentric cylinders has many engineering applications using rotating machinery components covering co-axial rotating heat pipes, cylindrical bearings, rotating membrane filters and there is lack in studying the flow in the basic of stationary cylinders such as bundled cylinders at offshore installation, risers, tube bundles in heat exchangers and mooring lines with the non-Newtonian fluids are more effective than the Newtonian fluids as we previously mentioned. An effort has been made to investigate the natural convection of non-Newtonian power law fluids in eccentric cylinders at different angles numerically for the parameters $10^3 \leq \mathrm{Ra} \leq 10^5$, $10 \leq \mathrm{Pr} \leq 10^3$, $0.6 \leq n \leq 1.4$, and $0 \leq \varepsilon \leq 0.9$, and an inclination angle, ϕ, from 0° to 90°.

Problem formulation

The schema of the physical domain of the present problem is shown in fig. 1. The inner eccentric cylinder is of radius R_i and the outer one is R_o. The flow is considered 2-D steady-state and the convection is laminar, the fluid is incompressible non-Newtonian power law fluid and the cylinders are eccentric. The internal wall of the inner cylinder is heated uniformly at constant temperature T_h while the outer one cooled isothermally at temperature T_c ($T_\mathrm{h} > T_\mathrm{c}$).

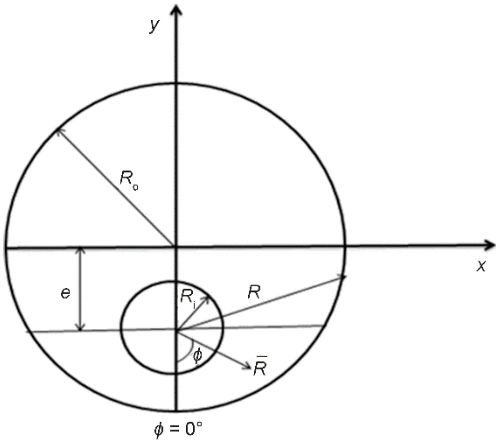

Figure 1. Description of the physical problem

We confess that the positive trend of the eccentricity is toward the bottom of the outer cylinder and the inner cylinder is able to be moved by an angle ϕ. Because of the temperature difference, a buoyancy induced flow results and the natural convection takes place within the power law in the gap. The Boussinesq approximation is used to calculate the buoyancy forces in the radial and angular directions. The equations that govern our flow are continuity, momentum and energy.

These equations are:

$$\frac{\partial u}{\partial x}+\frac{\partial v}{\partial y}=0 \tag{1}$$

$$\rho u\frac{\partial u}{\partial x}+\rho v\frac{\partial u}{\partial y}=-\frac{\partial P}{\partial x}+\mu\left(\frac{\partial^2 u}{\partial x^2}+\frac{\partial^2 u}{\partial y^2}\right) \tag{2}$$

$$\rho u\frac{\partial v}{\partial x}+\rho v\frac{\partial v}{\partial y}=-\frac{\partial P}{\partial y}+\mu\left(\frac{\partial^2 v}{\partial x^2}+\frac{\partial^2 v}{\partial y^2}\right)+\rho \mathrm{g}\beta(T-T_\mathrm{c}) \tag{3}$$

$$\rho C_p u\frac{\partial T}{\partial x}+\rho C_p v\frac{\partial T}{\partial y}=k\left(\frac{\partial^2 T}{\partial x^2}+\frac{\partial^2 T}{\partial y^2}\right) \tag{4}$$

These equations are used for the following boundary conditions:

$$R = R_\mathrm{i} \qquad u = v = 0 \qquad T = T_\mathrm{h} \tag{5}$$

$$R = R_\mathrm{o} \qquad u = v = 0 \qquad T = T_\mathrm{c} \tag{6}$$

$$\phi = 0 \qquad u = v = 0 \qquad \frac{\partial T}{\partial R} = 0 \tag{7}$$

$$\phi = 2\pi \qquad u = v = 0 \qquad \frac{\partial T}{\partial R} = 0 \tag{8}$$

The temperature when the fluid properties are taken is at $T_\mathrm{f} = (T_\mathrm{h} + T_\mathrm{c})/2$.

The apparent viscosity for a power law fluid in the Cartesian co-ordinate is:

$$\mu_\mathrm{a}=K\left\{\left[2\left(\frac{\partial u}{\partial x}\right)^2+\left(\frac{\partial v}{\partial y}\right)^2\right]+\left(\frac{\partial v}{\partial x}+\frac{\partial u}{\partial y}\right)^2\right\}^{(n-1)/2} \tag{9}$$

The previous form of the viscosity is the most common and the easiest one to simulate the viscosity with, where μ_a is the apparent viscosity of the power law, K – the consistency parameter, and n – the power law index. The n is the responsible for the type of fluid with $n = 1$: Newtonian fluid, the Newtonian fluids have a dynamic coefficient of viscosity K, $n \leq 1$: the fluid is pseudo-plastic fluid, and $n \geq 1$: the fluid is dilatant fluid.

The Rayleigh and Prandtl numbers are:

$$\mathrm{Ra}=\frac{\rho^2 \mathrm{g}\beta C_p \Delta T L^3}{\mu_\mathrm{ref} k^2}, \quad \mathrm{Pr}=\frac{\mu_\mathrm{ref} C_p}{k} \tag{10}$$

where Ra represents the ratio of the strengths of thermal transport due to buoyancy to thermal conduction, and Pr represents the ratio of the viscous boundary-layer to thermal boundary-layer thicknesses. For power law fluids, the viscosity is varying with the flow so we need to put a reference viscosity, μ_{ref}, which was mentioned in eqs. (4), (9), and (10). This viscosity is defined based on a characteristic shear rate, γ, which itself can be scaled as $\gamma = u_{\mathrm{scale}}/L$. This scaled viscosity is $u_{\mathrm{scale}} = \alpha/L$.

$$\mu_{\mathrm{ref}} = K\gamma^{n-1} = K\left(\frac{\alpha}{L^2}\right)^{n-1} \tag{11}$$

The previous equation is used for analyzing the natural convection as a representative value, but with the velocity scale we are able to write Rayleigh and Prandtl numbers as functions of the quantities g, $\beta, K, \rho, \alpha, k$, and L.

$$\mathrm{Ra} = \frac{\rho^2 \mathrm{g}\beta\Delta T L^{2n+1}}{\alpha^n K}, \quad \mathrm{Pr} = \frac{KL^{2-2n}}{\rho\alpha^{2-n}} \tag{12}$$

The local and mean Nusselt numbers are:

$$\mathrm{Nu_L} = -\frac{\partial\theta}{\partial R}, \qquad \mathrm{Nu_{ave}} = \frac{1}{2\pi}\int_0^{2\pi} \mathrm{Nu_L}\,\mathrm{d}\phi \tag{13}$$

Numerical approach and procedure

The previous governing equations which are applied for their boundary conditions were numerically solved using ANSYS-CFX package version 16. This commercial code is able to solve the differential equations by converting them into algebraic equations using finite volume method (FVM), the SIMPLE algorithm which introduced by Patankar [35] was used for these equations and the second order upwind schemes were used to reduce the numerical errors. The steady laminar model was used for all the simulations. The grid system is uniform in the angular direction but not uniform in the radial direction. It's thicker near the inner and outer surfaces of the cylinders as the fig. 2 illustrates. It is expected that the solution converge when the residuals of continuity and momentum are less than 10^{-9} and the residuals of energy is nearly 10^{-6}.

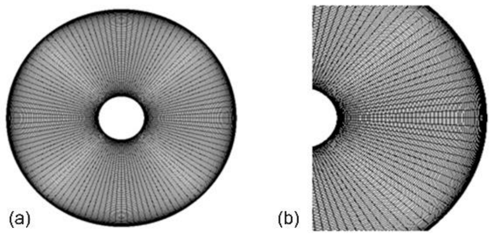

Figure 2. (a) Schematic of the numerical domain, (b) Part of the numerical domain

Code validation

To guarantee that our current data are in the right trail with the previous works, a validation test was conducted, and the results have been compared with some set of works which were performed on natural convection. The well reference of natural convection by Kuehn and Goldstein [2] for the dimensionless temperature, Abu-Nad *et al.* [9] and Matin and Khan [15] for Nusselt number *vs.* Rayleigh number. These comparisons are illustrated in the figs. 3-5. It is obvious that our results are congruous to theirs except for the numerical errors.

Now, to deepen in the investigations, our results have been checked for the cases of pseudo-plastic and dilatant fluids ($n < 1$ and $n > 1$, respectively) with the ones of Turan *et al.* [24] and Matin and Khan [15]. Table 1 presents the comparison.

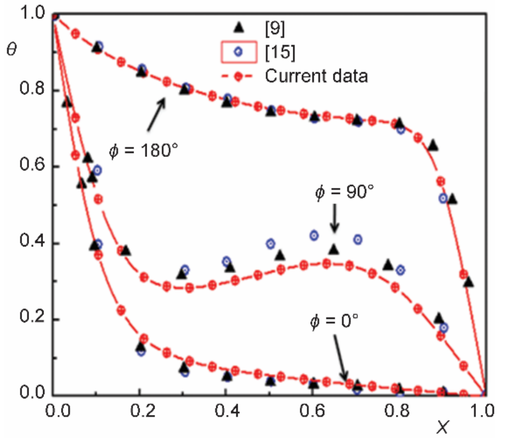

Figure 3. Comparison between the present work for the dimensionless temperature and the results in [9] and [15] for $e = 0$, $n = 1$, $RR = 2.6$, $Ra = 4.7 \cdot 10^4$ and $Pr = 0.706$

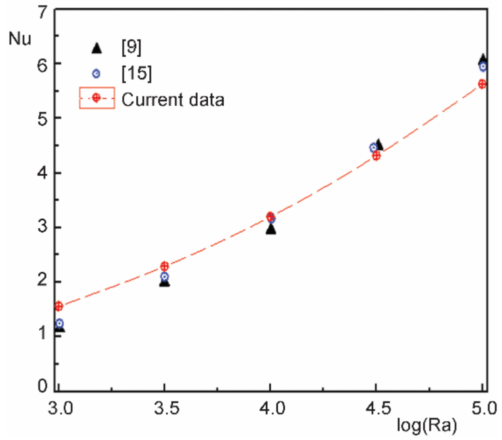

Figure 4. Comparison between the present work for the Nu and the results in [9] and [15] for $e = 0$, $n = 1$, $RR = 2.5$, and $Pr = 0.7$

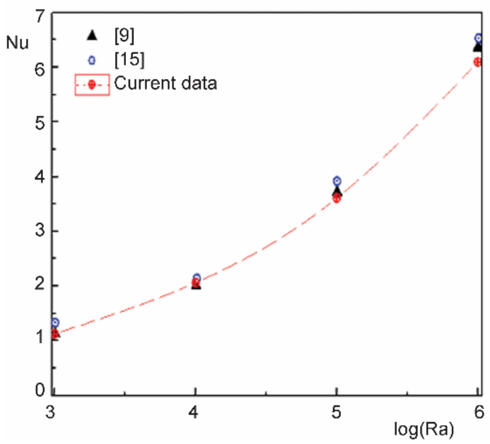

Figure 5. Comparison between the current data of the Nu and the results in [2] and [15] for $e = 0$, $n = 1$, $RR = 2.6$, and $Pr = 0.7$

Table 1. Comparison of the average Nusselt number between our work (current data) and the results in [24] and [15]

	Ra	Nu		
		$n = 0.6$	$n = 1.0$	$n = 1.4$
Current data	10^4	5.69545	2.27263	1.34699
	10^5	12.4609	4.70245	2.42811
[15]	10^4	5.76019	2.38638	1.35504
	10^5	13.06722	4.69312	2.28356
[24]	10^4	5.70903	2.40512	1.35514
	10^5	12.98500	4.72576	2.28945

Results and discussions

The effects of buoyancy force (laminar natural convection) on the fluid-flow and the heat transfer characteristics are presented. Effects of Ra, Pr, ε, ϕ, and n on the average Nusselt number are examined as well.

Discussing the isotherms and streamlines

Figures 6 and 7 represent isotherms and streamlines for the various parameters of Ra, Pr, *n*, and ε. These figures show the effects of the previous parameters on the flow field (thermal field). From the figures one can see that when $\phi = 0$ the isotherms and streamlines are symmetric about the *y* axis of the inner cylinder for all the cases. Also, there is a thermal plume around the inner cylinder and in the lower portion of the annulus the flow is stable and fully stratified in which we call a stagnant region where there is almost no heat transfer (in this region we cannot find any temperature contours and the flow does not recirculate in it) for all the cases. Moreover, one can see that when we increase the power law index *n* (from the shear thinning behavior to the shear thickening behavior) at the same values of Ra and Pr, the thermal plume

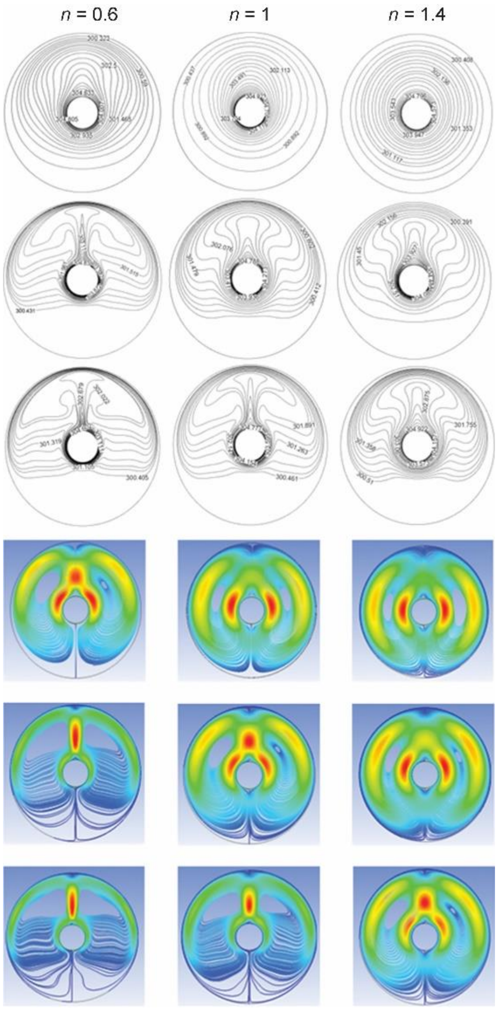

Figure 6. Isotherms (up) and streamlines (down) for Pr = 100, ε = 0, for different values of *n* and Ra; Ra = 10^3 (first row), Ra = 10^4 (second row), Ra = 10^5 (third row)

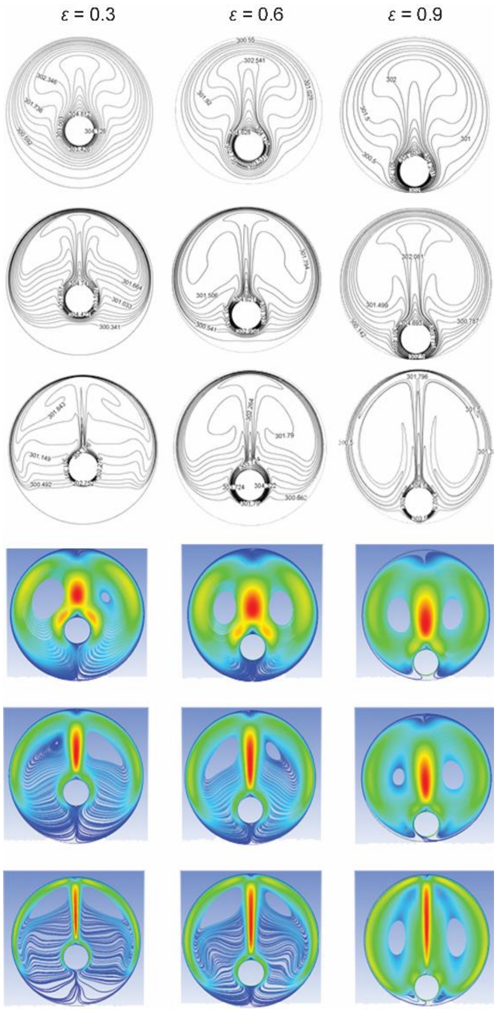

Figure 7. Isotherms (up) and streamlines (down) for Pr = 100, *n* = 0.6, ϕ = 0° for different values of ε and Ra; Ra = 10^3 (first row), Ra = 10^4 (second row), Ra = 10^5 (third row)

reduces which is a sign that pseudo-plastic fluids are better than the others in transferring the heat. At low Rayleigh numbers the flow pattern depends essentially on n (the patterns of isotherms for dilatant fluids are very close to those of the heat transfer by conduction).

The figures also show the effects of Rayleigh number on the heat and flow field. It is evident that the thermal plume region extends with increasing the Rayleigh number and this means that the strength of buoyancy force is affected and consisted of the Rayleigh values. At low Rayleigh number the shape of isotherms for pseudo-plastic, Newtonian and dilatant fluids are virtually alike because the thermal transport occurs almost by conduction and the heat transfer regime is by conduction more than convection. In addition, isotherms are parallel distributed to the cylinders (taking the concentric shape case) so natural convection is very weak compared with conduction. Also, one can see that the streamlines have weak values (here the effects of n can not be well seen, it might be seen clearly in dilatant fluids where their Nusselt number is very weak). When Rayleigh number gets bigger ($\mathrm{Ra} \geq 10^4$) conduction still the dominant for dilatant fluids but not anymore for the other fluids, isotherms move up toward the outer cylinder and change their shape becoming well spread not parallel distributed and for streamlines the main eddy moves upward to the outer cylinder (this phenomenon is clearly seen in pseudo-plastic fluids then the Newtonian then dilatant fluids which means that the fluid movement is rapid in pseudo-plastic fluids then the Newtonian and then dilatant fluids). When Rayleigh number gets to higher values ($\mathrm{Ra} \geq 10^5$) the natural convection takes place in the dilatant fluid, the main eddy starts to deform and change its shape from the bean shape to the stretch (airfoil) shape.

In this part the effect of eccentricity is depicted and showed in fig. 7. From the figures it is obviously seen that the eccentricity has effects on heat transfer, the gap between the south part of the inner cylinder and the outer one becomes tighter and from here we may say that the fluid can not have liberty to circulate in this region. It is observed that when we raise the value of eccentricity the thermal plume augments at the same set of Rayleigh number, n, and ϕ. The eccentricity causes the flow in the down area (the flow below the inner cylinder) in which we know as the stagnant fluid to reduce giving away freedom to the thermal plume to spread and extend more and more which boosts the convective flow to become more intensive. This last one is bigger in the vertical case compared with the others because in this case it takes big part from the stagnant region and when we increase the angle, ϕ, the distance between the north part of the inner cylinder and the outer one (the thermal plume region) diminishes which causes the convective heat transfer to reduce.

Effects of Rayleigh and Prandtl numbers, ε, ϕ, and n on the mean Nusselt number

Figures 8-10 illustrate the variation of the average Nusselt number as a function of different set of parameters power law index, n, Rayleigh and Prandtl numbers, ε at ϕ = 0°, 45°, and 90°, respectively. From the figures one can see that when the power law index, n, gets bigger (from the shear thinning behavior to the shear thickening behavior) the curves of the Nusselt number go down which is a signal for the low heat transfer in this case. Also, it is observed that the Nusselt number for pseudo-plastic fluids is higher than that of the Newtonian and is higher than that of the dilatant fluids and this boosts the fact of pseudo-plastic fluids are better than Newtonian and dilatant fluids in cooling and heating purposes. Furthermore, one can see that the Nusselt number incredibly affected by the Rayleigh number because when Rayleigh augments all the curves of the Nusselt number go up which means that the Nusselt number depends on the Rayleigh number, this is because Rayleigh number strengthens the buoyancy force that results from the gradient in density (difference of density) and consequen-

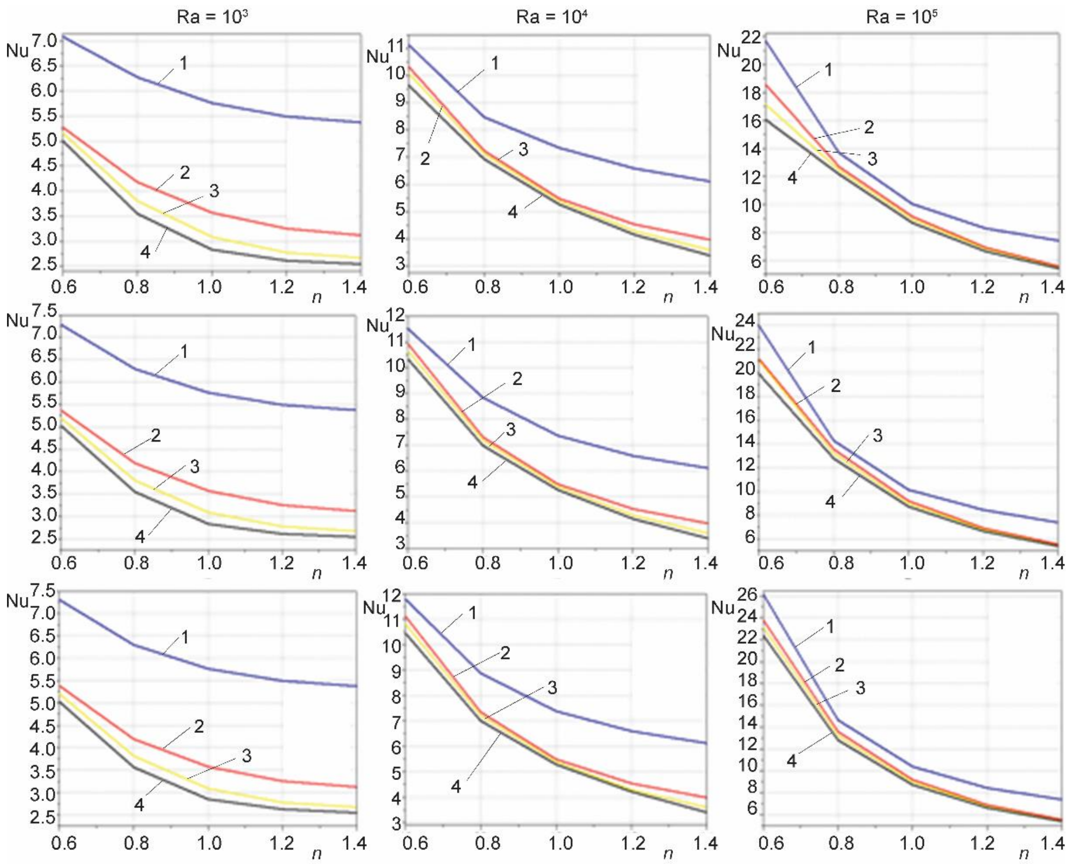

Figure 8. Mean Nusselt number *vs.* power law index at $\phi = 0°$ for different parameters of Ra, ε, and Pr; Pr = 10 (first row), Pr = 100 (second row), Pr = 1000 (third row);
1 – ε = 0.9, 2 – ε = 0.6, 3 – ε = 0.3, 4 – ε = 0

tly, with decreasing *n* these effects become more pronounced, so the effect of convection in pseudo-plastic fluids are more evident than the others and at low Rayleigh num-bers conduction becomes the dominant mode of heat transfer. This phenomenon is clearly seen in dilatant fluids than the others and when Rayleigh number gets bigger (Ra $\geq 10^4$) the effect of convection begins to appear. Then, the figures show that Prandtl number has almost no effect on the heat transfer (on the Nusselt number) this is because Prandtl number effects are more on the hydrodynamic boundary-layer thickness than the thermal boundary-layer thickness. Effects of Prandtl number can be a bit seen only for pseudo-plastic fluids at high Rayleigh numbers (Ra $\geq 10^5$) but not for the other fluids so in this situation we can say that the Prandtl number affects only the viscous and thermal diffusion forces in the boundary-layer but does not affect the thermal boundary-layer thickness. We may deduce the Nusselt number is autonomous of Prandtl number.

From the figures one can see that the Nusselt number affected by the eccentricity value. It is obvious that when the eccentricity increases the Nusselt number increases especially for pseudo-plastic fluids when *n* is very small ($n \leq 0.6$) or dilatant fluids when *n* is very big ($n \geq 1.4$) at low Rayleigh numbers. That is because the thermal plume gets more freedom to extend above the inner cylinder and the gap below the inner cylinder shrinks more (the space

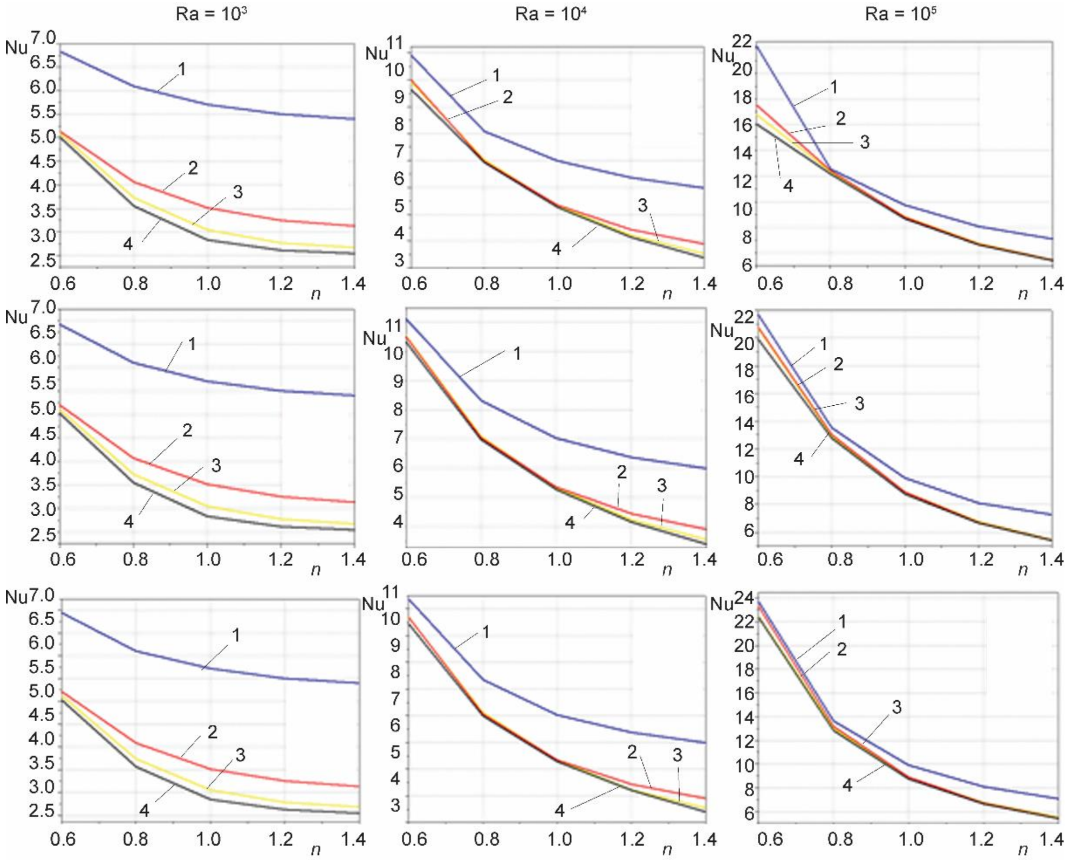

Figure 9. Mean Nusselt number *vs.* power law index at ϕ = 45° for different parameters of Ra, ε, and Pr; Pr = 10 (first row), Pr = 100 (second row), Pr = 1000 (third row);
1 – ε = 0.9, 2 – ε = 0.6, 3 – ε = 0.3, 4 – ε = 0

where we can find the stratified fluid). Still, as Rayleigh is low the conduction is the dominant mode of heat transfer because the buoyancy force is too weak that can not let the thermal plume to spread. Another phenomenon needs to be explained here is when ϕ = 90° at low Rayleigh numbers the increase of eccentricity causes the heat transfer to reduce for pseudo-plastic fluids because the influence of eccentricity on heat transfer is greater than the buoyancy force except for the big values of eccentricity ε = 0.9 where the collision between the hot and cold fluid in the upright trend of the eccentricity from the gravity force is able to drive the buoyancy force and make it stronger. When Rayleigh gets bigger (Ra $\geq 10^4$) the convection mode begins to be the driving mode of heat transfer and this effect starts to appear in dilatant fluids ($n \geq 1.4$) in which the eccentricity causes them to reduce their resistances and overwhelmed all the fluids (pseudo-plastic, Newtonian and dilatant fluids) when Rayleigh is big enough (Ra $\geq 10^5$) to produce a great buoyancy force.

The figures also show the effects of angle ϕ on the heat transfer rate. From the figures one can see that when ϕ increases from the vertical orientation (ϕ = 0°) to the horizontal orientation (ϕ = 90°) the values of the Nusselt number diminish which is a sign for diminishing the heat transfer here, these effects are clearly seen at low Rayleigh numbers (Ra $\leq 10^4$) at ε = 0.9.

Furthermore, when Rayleigh is high (Ra $\geq 10^5$) these effects become less strong especially between the cases $\phi = 45°$ and $\phi = 90°$. So, one can deduce here that the best case of heat transfer occurs at $\phi = 0°$.

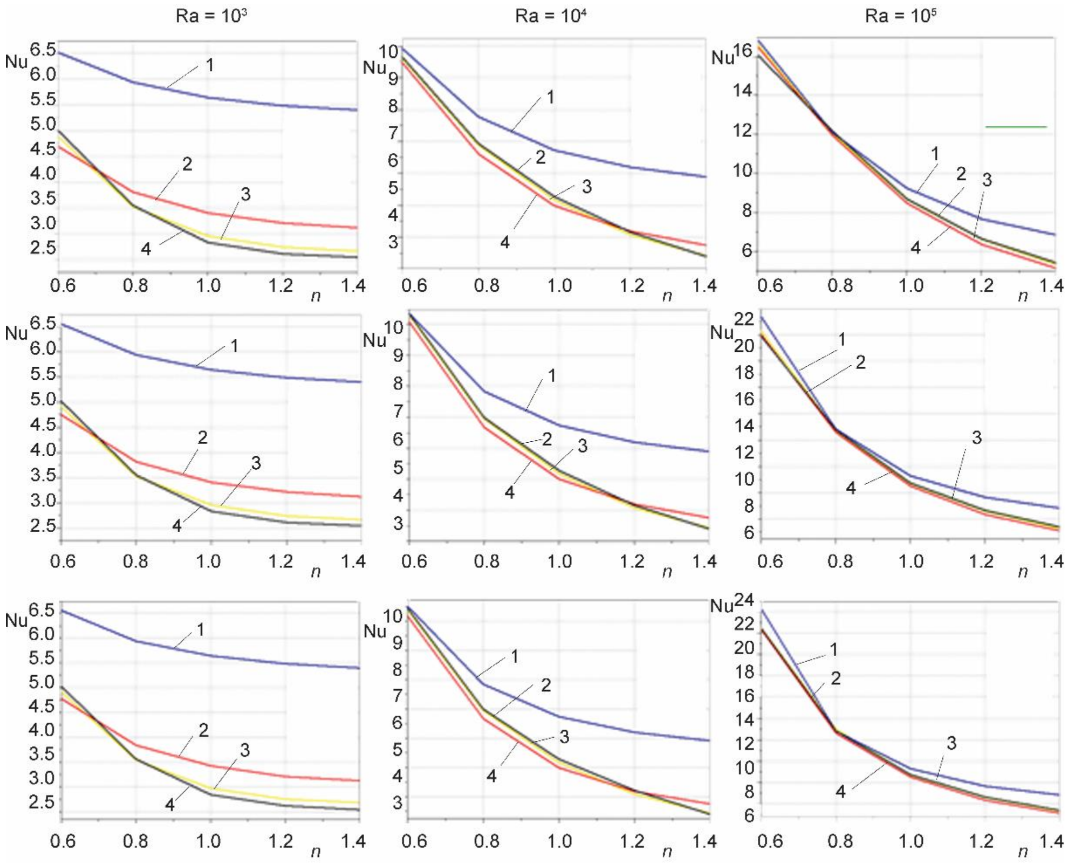

Figure 10. Mean Nusselt number *vs.* power law index at $\phi = 90°$ for different parameters of Ra, ε, and Pr; Pr = 10 (first row), Pr = 100 (second row), Pr = 1000 (third row);
1 – ε = 0.9, 2 – ε = 0.6, 3 – ε = 0.3, 4 – ε = 0

Conclusions

The 2-D steady-state natural convection of non-Newtonian power law fluid has been analyzed numerically. The results have come from the parameters $10^3 \leq \text{Ra} \leq 10^5$, $10 \leq \text{Pr} \leq 10^3$, $0.6 \leq n \leq 1.4$, $0 \leq \varepsilon \leq 0.9$ and an inclination angle ϕ from 0° up to 90°. The model of Ostwald-de Waele used here to simulate our non-Newtonian fluid. As a result, from the above survey we may extract the following:

- The Nusselt number affected by the power law index n when all the other parameters kept the same. This effect is more vigorous for pseudo-plastic fluids than the others at high Rayleigh numbers.
- The Nusselt number is not affected by Prandtl number except for pseudo-plastic fluids when Ra values are considerable (Ra $\geq 10^5$) at the same values of ϕ and ε. These effects are really small to be negligible.

- The Nusselt number is depends on the Rayleigh number in which (this last one) drives the strengths of buoyancy force and when it sets with $\varepsilon = 0.9$ at $\phi = 0°$ (the vertical case) The best heat transfer could be found.
- The Nusselt number is affected by the eccentricity rate wherein we increase it the Nusselt number grows up at the same set of Ra, Pr, and n, excluding when n is very weak for pseudo-plastic fluids ($n \leq 0.6$) or very large for dilatant fluids ($n \geq 1.4$) at $\varepsilon = 0.6$ and $\phi = 90°$ for low Rayleigh numbers (Ra $\leq 10^4$).
- The Nusselt number affected by the angle ϕ wherein we increase ϕ from the vertical state to the horizontal state the Nusselt number decreases. The best case among them all is at $\phi = 0°$.

Nomeclature

C_p – specific heat capacity, [Jkg^{-1}K^{-1}]
e – distance between the centers of cylinders, [m]
g – gravity acceleration, [ms^{-2}]
K – consistency index of the power-law
k – thermal conductivity, [Wm^{-1}K^{-1}]
L – characteristic length (= $R_o - R_i$), [m]
n – power-law index, [–]
Nu$_{ave}$ – average Nusselt number
P – pressure, [Pa]
Pr – Prandtl number, [–]
Ra – Rayleigh number, [–]
R – radius, [m]
R_i – radius of the inner cylinder, [m]
R_o – radius of the outer cylinder, [m]
$\bar{R}$ – dimensionless radius, [–]
RR – hydraulic radius ratio, [R_o/R_i]
T – temperature, [K]
T_h – inner cylinder temperature, [K]
T_c – outer cylinder temperature, [K]
ΔT – difference between hot and cold temperatures (= $T_h - T_c$)
u, v – radial and tangential velocities, [ms^{-1}]
x, y – cartesian co-ordinates

Greek symbols

α – thermal diffusivity, [m^{2}s^{-1}]
β – volume coefficient of expansion, [K^{-1}]
γ – rate of strain tensor, [s^{-1}]
ε – eccentricity factor, [–]
θ – dimensionless temperature, [–]
μ – dynamic viscosity, [Nsm^{-2}]
μ_a – apparent viscosity, [–]
μ_{ref} – reference viscosity, [Nsm^{-2}]
ρ – density, [kgm^{-3}]
ϕ – orientation angle, [°]

References

[1] Mack, L. R., Bishop, E. H., Natural Convection between Horizontal Concentric Cylinders for Low Rayleigh Numbers, *Quart. J. Mech Appl Math, 21* (1968), 2, pp. 223-241
[2] Kuehn, T. H., Goldstein R. J., An Experimental and Theoretical Study of Natural Convection in the Annulus between Horizontal Concentric Cylinders, *J. Fluid Mechanics, 74* (1976), 4, pp. 695-719
[3] Char, M. I., Lee, G. C., Maximum Density Effects on Natural Convection of Micropolar Fluids between Horizontal Eccentric Cylinders, *Int. J. Eng. Sci., 36* (1998), 2, pp. 157-169
[4] Kim, G. B., *et al.*, Transient Buoyant Convection of a Power-Law Non-Newtonian Fluid in an Enclosure, *Int. J. Heat Mass Transfer, 46* (2003), 19, pp. 3605-3617
[5] Naimi, M., *et al.*, Natural Convection of Non-Newtonian Power Law Fluids in a Shallow Horizontal Rectangular Cavity Uniformly Heated from Below, *Heat Mass Transfer, 41* (2005), 3, pp. 239-249
[6] Sakr, R. Y., *et al.*, Experimental and Numerical Investigation of Natural Convection Heat Transfer in Horizontal Elliptic Annuli, *Int. J. Che Reactor Eng., 6* (2008), 1, pp. 1-29
[7] Kumar, R., Study of Natural Convection in Horizontal Annuli. *Int. J. Heat Mass Transfer, 31* (1988), 6, pp. 1137-1148
[8] Yigit, S., *et al.*, Numerical Investigation of Laminar Rayleigh-Benard Convection of Power-Law Fluids in Square Cross-Sectional Cylindrical Annular Enclosures, *Int Commun in Heat Mass Transfer, 78* (2016), Nov., pp. 112-120
[9] Abu-Nada, E., *et al.*, Natural Convection Heat Transfer Enhancement in Horizontal Concentric Annuli Using Nanofluids, *Int Commun in Heat Mass Transfer, 35* (2008), 5, pp. 657-665
[10] Chamkha, A. J., Ben-Nakhi, A., Natural Convection in Inclined Partitioned Enclosures, *Heat Mass Transfer, 42* (2006), 4, pp. 311-321
[11] Ben-Nakhi, A., Chamkha, A. J., Conjugate Natural Convection in a Square Enclosure with Inclined Thin Fin of Arbitrary Length, *Int. J. Thermal Sci, 46* (2007), 5, pp. 467-478

[12] Khezzar, L., *et al.*, Natural Convection of Power Law Fluids in Inclined Cavities, *Int. J. Thermal Sci, 53* (2012), Mar., pp. 8-17
[13] Parvin, S., *et al.*, Thermal Conductivity Variation on Natural Convection Flow of Water-Alumina Nanofluid in an Annulus, *Int. J. Heat Mass Transfer, 55* (2012), 19-20, pp. 5268-5274
[14] Chhabra, R. P., *et al.*, Free Convection from a Heated Circular Cylinder in Bingham Plastic Fluids, *Int. J. Therm. Sci., 83* (2014), Sept., pp. 33-44
[15] Matin, M. H., Khan, W. A., Laminar Natural Convection of Non-Newtonian Power-Law Fluids between Concentric Circular Cylinders, *Int Commun in Heat Mass Transfer, 43* (2013), Apr., pp. 112-121
[16] Turki, S., *et al.*, Numerical Prediction of Flow and Heat Transfer of Power-Law Fluids in a Plane Channel with a Built-in Heated Square Cylinder, *Int. J. Heat Mass Transfer, 53* (2010), 23-24, pp. 5420-5429
[17] Chamkha, A. J., *et al.*, Numerical Analysis of Unsteady Conjugate Natural Convection of Hybrid Water-Based Nanofluid in a Semi-Circular Cavity, *J. Therm Sci & Eng Apps, 9* (2017), 4, pp. 1116-1127
[18] Chamkha, A. J., *et al.*, Mixed Convection Heat Transfer of Air inside a Square Vented Cavity with a Heated Horizontal Square Cylinder, *Num Heat Transfer, Part A: Applications, 59* (2011), 1, pp. 58-79
[19] Khanafer, K., Chamkha, A. J., Mixed Convection within a Porous Heat Generating Horizontal Annulus, *Int. J. Heat Mass Transfer, 46* (2003), 10, pp. 1725-1735
[20] Matin, M. H., *et al.*, Natural Convection of Power-Law Fluid between Two-Square Eccentric Duct Annuli, *J. Non-Newtonian Fluid Mech, 197* (2013), July, pp. 11-23
[21] Alawi, O. A., *et al.*, Natural Convection Heat Transfer in Horizontal Concentric Annulus between Outer Cylinder and Inner Flat Tube Using Nanofluid, *Int Commun in Heat Mass Transfer, 57* (2014), Oct., pp. 65-71
[22] Parvin, S., Chamkha, A. J., An Analysis on Free Convection Flow Heat Transfer and Entropy Generation in an Odd-Shaped Cavity Filled with Nanofluid, *Int Commun in Heat Mass Transfer, 54* (2014), May, pp. 8-17
[23] Chamkha, A. J., *et al.*, Bouzerzour, A., Natural Convective Nanofluid Flow in an Annular Space between Confocal Elliptic Cylinders, *J. Thermal Sci Eng Applications, 9* (2017), 1, pp. 1-9
[24] Turan, O., *et al.*, Laminar Natural Convection of Power-Law Fluids in a Square Enclosure with Differentially Heated Side Walls Subjected to Constant Temperatures, *J. Non-Newtonian Fluid Mech, 166* (2011), 17-18, pp. 1049-1063
[25] Chamkha, A. J., Ismael, M. A., Natural Convection in Differentially Heated Partially Porous Layered Cavities Filled with a Nanofluid, *Num Heat Transfer, Part A: Applications, 65* (2014), 11, pp. 1089-1113
[26] Ismael, M. A., Chamkha, A. J., Conjugate Natural Convection in a Differentially Heated Composite Enclosure Filled with a Nanofluid, *J. Porous Media, 18* (2015), 7, pp. 699-716
[27] Chhabra. R. P., *et al.*, Effect of Aiding-Buoyancy on Mixed Convection from a Heated Cylinder in Bingham Plastic Fluids, *J. Non-Newtonian Fluid Mech, 220* (2015), June, pp. 3-21
[28] Nasrin, R., *et al.*, Effect of Viscosity Variation on Natural Convection Flow of Water-Alumina Nanofluid in an Annulus with Internal Heat Generation, *Heat Transfer-Asian Research, 41* (2012), 6, pp. 536-552
[29] Tayebi, T., Chamkha, A. J., Free Convection Enhancement in an Annulus between Horizontal Confocal Elliptical Cylinders Using Hybrid Nanofluids, *Num Heat Transfer, Part A: Applications, 71* (2017), 10, pp. 1159-1173
[30] Chamkha, A. J., Ismael, M. A., Conjugate Heat Transfer in a Porous Cavity Heated by Triangular Thick Wall, *Num Heat Transfer, Part A: Applications, 63* (2012), 2, pp. 144-158
[31] Chamkha, A. J., Ismael, M. A., Conjugate Heat Transfer in a Porous Cavity Filled with Nanofluids and Heated by Triangular Thick Wall, *Int. J. Thermal Sci, 67* (2013), May, pp. 135-151
[32] Selimefendigil, F., Chamkha, A. J., Natural Convection of a Hybrid Nanofluid-Filled Triangular Annulus with an Openning, *Computational Thermal Sciences, 8* (2016), 6, pp. 555-566
[33] Oztop, H. F., *et al.*, Natural Convection in Wavy Enclosures with Volumetric Heat Sources, *Int. J. Thermal Sci, 50* (2011), 4, pp. 502-514
[34] Abu-Nada, E., Chamkha, A.J., Mixed Convection Flow of a Nanofluid in a Lid-Driven Cavity with a Wavy Wall, *Int Commun in Heat Mass Transfer, 57* (2014), Oct., pp. 36-47
[35] Patankar, S.V, *Numerical Heat Transfer and Fluid Flow*, McGraw Hill, New York, USA, 1980

Paper submitted: August 5, 2019
Paper revised: September 24, 2019
Paper accepted: October 30, 2019
© 2021 Society of Thermal Engineers of Serbia.
Published by the Vinča Institute of Nuclear Sciences, Belgrade, Serbia.
This is an open access article distributed under the CC BY-NC-ND 4.0 terms and conditions.